JOURNAL OF AIRCRAFT
Vol. 48, No. 2, March–April 2011

# Morphing Aircraft Sizing Using Design Optimization

William A. Crossley,* Michael D. Skillen,† Joshua B. Frommer,‡ and Brian D. Roth§
*Purdue University, West Lafayette, Indiana 47907-2045*

DOI: 10.2514/1.C031180

**This paper summarizes design optimization approaches for sizing a morphing aircraft for which the wing can make significant shape changes in flight. The approaches include single-level problems solved by gradient-free and gradient-based optimizers and a multilevel problem solved by gradient-based optimizers; of these, the multilevel approach proved most efficient. In the multilevel approach, a top-level problem minimizes the aircraft gross weight using reference design variables ($T/W$, $S$, AR, $t/c$, $\Lambda$, and $\lambda$), along with morphing limit variables describing the maximum shape change as a function of the reference geometry (e.g., $\Delta b$, $\Delta c$, and $\Delta\Lambda$). A sublevel problem for each mission segment determines an optimal wing-shape scheduling that minimizes fuel consumption, satisfies performance constraints, and operates within the geometric domain prescribed by the top-level problem. While the empty-weight buildup uses traditional predictors for fixed-geometry components, the wing weight prediction uses a parametric equation derived from structural optimization studies of morphing wings. The multilevel optimization approach then sizes an aircraft for which the wing can change sweep and root chord length, demonstrating: 1) the optimal wing-shape scheduling and maximum shape change for the morphing strategy, 2) the approach's ability to facilitate continuous morphing during mission segment analysis, and 3) improved effectiveness over previous single-level morphing aircraft sizing approaches.**

## Nomenclature

| | | |
|---|---|---|
| AR | = | aspect ratio |
| $b$ | = | wing span |
| $c$ | = | wing chord |
| $C_L$ | = | wing lift coefficient |
| $(C_L)_{\max}$ | = | maximum lift coefficient |
| $c_{\text{mac}}$ | = | wing mean aerodynamic chord |
| $c_{\text{root}}$ | = | wing root chord |
| $d_{\text{land}}$ | = | landing distance |
| $d_{\text{TO}}$ | = | takeoff distance |
| $F$ | = | morphing-wing template function |
| $f$ | = | objective function |
| $g_c$ | = | compatibility constraint |
| $g_j$ | = | performance or flight envelope constraint |
| $i$ | = | design variable index |
| $j$ | = | performance of flight envelope constraint index |
| $k$ | = | mission-leg or subsegment index |
| $M$ | = | Mach number |
| $m$ | = | number of mission legs in the aircraft design mission |
| $M_{\text{dash}}$ | = | dash Mach number |
| $P_S$ | = | specific excess power |
| $S$ | = | wing planform area |
| $t/c$ | = | wing thickness-to-chord ratio |
| $T_{\text{SL}}$ | = | installed sea-level static thrust |
| $T_{\text{SL}}/W_0$ | = | thrust-to-weight ratio |
| $V_{\text{approach}}$ | = | approach velocity |
| $V_{\text{stall}}$ | = | stall velocity |
| $W_{\text{fuel}}$ | = | design mission fuel weight |
| $(W_{\text{fuel}})_k$ | = | mission-leg or subsegment fuel weight |
| $W_G$ | = | calculated gross weight |
| $W_{\text{wing}}$ | = | wing component weight |
| $W_0$ | = | gross weight, initial guess, or design variable |
| $W_0/S$ | = | wing loading |
| $\mathbf{X}$ | = | top-level design variable vector |
| $\mathbf{x}$ | = | design variable vector |
| $\mathbf{X}^{\text{ref}}$ | = | subset of $\mathbf{X}$ containing reference wing-geometry design variables |
| $\mathbf{X}^{\text{ub}}$ | = | subset of $\mathbf{X}$ containing maximum morphing shape-change design variables |
| $\mathbf{Y}$ | = | wing-geometry descriptor vector |
| $\Delta b$ | = | change in wingspan |
| $\Delta c$ | = | change in wing chord |
| $\Delta c_{\text{root}}$ | = | change in wing root chord |
| $\Delta\Lambda$ | = | change in wing sweep |
| $\Delta\Lambda_{\text{LE}}$ | = | change in wing leading-edge sweep |
| $\varepsilon$ | = | tolerance or cushion value |
| $\Lambda$ | = | wing sweep |
| $\lambda$ | = | wing taper ratio |
| $\Lambda_{\text{LE}}$ | = | wing leading-edge sweep |
| $\boldsymbol{\xi}$ | = | sublevel optimization design variables describing the morphed wing state |
| $()_{\text{ref}}$ | = | reference wing-geometry variable |
| $()_{\text{ub}}$ | = | morphing upper-bound variable |
| $()^L$ | = | variable lower-bound limit |
| $()^U$ | = | variable upper-bound limit |

Presented as Paper 2008-0166 at the 46th AIAA Aerospace Sciences Meeting and Exhibit, Reno, NV, 7–10 January 2008; received 14 July 2010; accepted for publication 24 September 2010. 

*Professor, School of Aeronautics and Astronautics, 701 West Stadium Avenue. Associate Fellow AIAA.

†Graduate Research Assistant, School of Aeronautics and Astronautics, 701 West Stadium Avenue; currently Lockheed Martin Aeronautics Company, Post Office Box 748, Mail Zone 9382, Fort Worth, Texas 76101. Member AIAA.

‡Graduate Research Assistant, School of Aeronautics and Astronautics, 701 West Stadium Avenue; currently Configuration Engineer, Boeing Commercial Aircraft Company, Post Office Box 3707, Mail Code 61-49, Seattle, Washington 98124-2207.

§Graduate Research Assistant, School of Aeronautics and Astronautics, 701 West Stadium Avenue; currently Assistant Professor, Walla Walla University, 204 South College Avenue, College Place, Washington 99324. Senior Member AIAA.

## I. Introduction

AIRCRAFT flight across a range of flight regimes requires compromise. The aircraft's shape and wing planform could cater to one crucial flight regime and suffer a performance penalty in offdesign conditions. Alternately, the shape and planform could balance performance to optimize a mission-wide measure of merit. In this case, performance is acceptable but nonoptimal for the individual design mission legs. An aircraft for which the wing can make significant planform and shape changes during flight could potentially improve performance in all flight regimes. This idea of a morphing aircraft is not new.

Swing-wing or variable sweep aircraft are morphing aircraft; the F-111 and F-14 are examples that reached production and entered military service. The ability to change wing sweep during flight enabled more efficient performance in both subsonic and supersonic flight regimes than a fixed-sweep wing.

In the 1980s, the Mission Adaptive Wing program [1] investigated the potential benefit of variable camber, in addition to variable sweep capabilities, to further improve flight performance. During the 1990s, developments in smart structures and active materials renewed interest in morphing aircraft. Defense Advanced Research Projects Agency's (DARPA's) Smart Aircraft and Marine System Projects Demonstration (SAMPSON) program investigated shape change of a tactical fighter inlet to improve performance in subsonic and supersonic flight [2]. In the 2000s, NASA's Aircraft Morphing project [3,4], DARPA's Smart Wing [5] and Morphing Aircraft Structures (MAS) [6] programs, and the U.S. Air Force Research Laboratory's Mission Adaptive Compliant Wing program [7] were some of the most visible initiatives to investigate these kinds of benefits. Focusing on changing the wing's planform, DARPA's MAS program goals included a 200% change in aspect ratio, a 50% change in wing area, and a 20° change in wing sweep. Phase II of the MAS program led to two flight-traceable morphing-wing concepts developed for wind-tunnel validation at representative flight conditions. Each concept successfully demonstrated large planform changes during testing. Illustrations of these concepts appear in Fig. 1. Lockheed Martin developed a folding-wing concept that varied span and effective sweep angle [8,9] (this appears as Fig. 1a). NextGen Aeronautics's concept varied root chord length and sweep angle [10] (this appears as Fig. 1b). NextGen Aeronautics also built two unmanned flying demonstrators with their variable-sweep/variable-root-chord morphing mechanisms [11].

With the advances in smart materials and adaptive structures, numerous efforts describe morphing mechanisms and devices. References [12–15] describe some specific efforts, while [16] attempts to survey a significant number of the proposed shape-change devices and mechanisms. These provide candidate actuation schemes for morphing aircraft, but these device-focused efforts generally do not address how to determine the type and extent of wing-shape changes best suited for the aircraft to perform a given mission.

Few publications describe how to relate the shape change of a morphing wing to vehicle-level improvements in performance and gross weight. Bowman et al. [17] provide a discussion of how wing planform changes impact aircraft performance characteristics; this includes using constraint diagrams to determine how changing wing loading ($W_0/S$) enables flight in two dissimilar regimes. However, the effort did not predict the gross weight and dimensions of a morphing aircraft. Bye and McClure [18] present an overview of the steps to design the folding-wing morphing aircraft (shown in Fig. 1a), which would operate in one of two discrete configurations: unfolded for loiter and cruise and folded for high-speed dash. Reference [18] mentions sizing studies for the folding-wing morphing aircraft and presents nondimensional carpet plots for a conventional aircraft asked to perform the same mission as the morphing aircraft. The description of the sizing approach does not contain enough information to determine if the approach could address a continuous planform shape change. Joshi et al. [19] use an intentionally simple approach to rapidly assess wing planform shapes having the most benefit for 11 different flight performance points. The results suggest a most promising strategy for in-flight planform changes, but the work does not size a morphing aircraft to complete a design mission.

a)

b)

**Fig. 1 Morphing-wing concepts from the DARPA MAS program: a) folding-wing concept (illustration from [37]) and b) variable sweep/variable-root-chord concept (illustration from [38]).**

For conceptual design of fixed-geometry aircraft, there are typically six significant design variables: 1) wing loading $W_0/S$ or wing planform area $S$, 2) thrust-to-weight ratio $T_{SL}/W_0$ or installed sea-level static thrust $T_{SL}$, 3) wing sweep $\Lambda$, 4) wing taper ratio $\lambda$, 5) wing thickness-to-chord ratio $t/c$, and 6) wing aspect ratio (AR) or span $b$; [20] calls these the basic six. An aircraft sizing algorithm will predict the weight, dimensions, and performance of the aircraft as a function of the design variables by using governing equations of flight, simple analysis models, and/or empirically based predictors. The result of the sizing process should be a set of design variable values that optimize an aircraft-level performance metric (often gross weight or cost) while satisfying mission requirements and side constraints. Carpet plots [21] are the traditional approach to identify the optimal design variable values; however, numerical optimization techniques can also facilitate this. References [22–25] present applications of mathematical optimization algorithms in the aircraft sizing process.

For morphing aircraft, the sizing algorithm and design variable set become more complex. Because the wing can accommodate some range of various outer mold line shapes during flight, performance and flight characteristics of the aircraft are a function of the wing-shape scheduling throughout the design mission. The sizing approach needs additional variables to model these wing-shape changes. Most existing aircraft sizing codes do not readily handle in-flight changes in wing geometry. Although these codes could simulate the aerodynamic effects of morphing by introducing new drag polars and/or other aerodynamic fudge factors during various mission segments, developing these would require analyses of all the possible wing shapes before running the sizing code, which is impractical. As an additional complexity, the morphing-wing weight will be a function of 1) the extent of the morphing actuation, 2) how the actuation affects structural stiffness and resulting load paths, and 3) the design load factors and aeroelastic response characteristics for each wing state. A wing with a larger extent of morphing will likely have an increased structural weight fraction. Therefore, to appropriately capture the aircraft-level benefits of morphing, the sizing must account for both the empty-weight impact of the morphing capability and the fuel weight impact of aerodynamic performance improvements from morphing.

Recognizing that existing sizing codes did not readily provide the necessary features to address the conceptual design of morphing aircraft, the authors of this paper, in varying combinations, conducted a sequence of investigations to determine the appropriate morphing aircraft sizing approach [26–29]. These efforts began with the perspective of providing a technology pull to identify high-impact uses of morphing and setting target requirements for further development of morphing devices, actuators, and effectors; as the work progressed, the perspective focused upon an approach that could represent a realizable morphing strategy. This paper summarizes these previous efforts and then expands upon the multilevel optimization approach of [29], which appears to be the most efficient for morphing aircraft sizing. The paper then demonstrates the latter method with three studies to size a morphing aircraft for which the wing can change sweep angle and root chord length.

## II. Morphing Aircraft Sizing Using Optimization Approaches

### A. Morphing as an Independent Variable

In an early effort, Roth et al. [26] and Roth and Crossley [27] introduced morphing as an independent variable. In this method, Roth et al. [26] developed an aircraft sizing code that incorporated morphing-wing capabilities. To describe aircraft geometry

throughout the design mission, the design variable set expanded from the basic six to include $S_k$, $\mathrm{AR}_k$, $(t/c)_k$, $\lambda_k$, and $\Lambda_k$, which describe the wing planform for each mission leg $k$, along with $T_{\mathrm{SL}}/W_0$. Thus, a morphing aircraft with a 10-leg design mission has nearly 10 times more variables than a fixed-geometry aircraft sizing problem. The increased number of variables rendered carpet-plot techniques intractable, motivating the use of an optimization approach. A representative morphing as an independent variable problem statement appears in Eqs. (1–5).

Minimize:

$$f(\mathbf{x}) = W_G(\mathbf{x}) \tag{1}$$

subject to

$$g_j(\mathbf{x}) = d_{\mathrm{TO}}(\mathbf{x}) \leq (d_{\mathrm{TO}})_{\mathrm{allow}} \tag{2}$$

$$g_j(\mathbf{x}) = M_{\mathrm{dash}}(\mathbf{x}) \geq (M_{\mathrm{dash}})_{\mathrm{min}} \tag{3}$$

$$x_i^L \leq x_i \leq x_i^U \tag{4}$$

where

$$\mathbf{x} = \{T_{\mathrm{SL}}/W_0 \quad S_1 \quad S_2 \quad \cdots \quad S_m \quad \mathrm{AR}_1 \quad \mathrm{AR}_2 \quad \cdots \quad \mathrm{AR}_m \quad (t/c)_1 \quad (t/c)_2 \quad \cdots \quad (t/c)_m \quad \lambda_1 \quad \lambda_2 \quad \cdots \quad \lambda_m \quad \Lambda_1 \quad \Lambda_2 \quad \cdots \quad \Lambda_m\} \tag{5}$$

The objective here was to minimize the gross weight of the aircraft. Equations (2) and (3) define a takeoff distance constraint and a dash Mach number constraint; the wing geometry that allows takeoff in a short distance is often poor for high-speed flight. If necessary, the formulation can incorporate other constraints appropriate to the mission. The design variable vector in Eq. (5) illustrates how the wing-geometry variables include one value for each design mission leg (the $m$ subscript indicates the number of the last leg).

Investigations revealed many nonclosure cases within the design space where the sizing code failed due to a numerical issue or the weight iterations never met an associated convergence tolerance. This discontinuous design space demanded a gradient-free search algorithm; a genetic algorithm (GA) provided this. However, the numerous nonclosure cases encountered in initial populations of the GA prompted a sequential application of the GA much like a trust region method. In this strategy, a fixed-geometry design that most closely met the design mission provided a starting point, and the basic variables could vary ±25% from this fixed-geometry design. The morphing variables describing the wing shape had slightly wider bounds, but the values assigned to upper and lower limits came largely from the authors' experience and observation while developing this approach. When the GA provided a solution for a minimum gross weight morphing aircraft, this solution provided a starting point for the subsequent runs. During the restart, the bounds of each morphing variable were adjusted based upon the previous solution, but the new upper and lower bounds were not allowed to exceed a set of absolute bounds. This sequential approach used five GA runs to obtain the optimal morphing aircraft description.

This effort addressed the major facets of the problem: incorporating shape-changing capabilities into the sizing process, developing a rudimentary weight prediction strategy for the morphing wing, and enabling a method to search for an optimal set of aircraft design variable values that described the shape of the wing in each mission leg. However, the approach was very computationally expensive and required significant user interpretation between sequential runs of the GA, motivating additional improvements.

### B. Enabling Continuous Optimization for Single-Level Morphing Aircraft Sizing Problems

Frommer and Crossley identified that the previous nonclosure cases emanated from the original problem formulation and, in response, developed the morphing-as-an-independent-variable strategy into a more computationally efficient form [28]. Because separate design variables modeled the wing state for each mission leg, the search algorithm could consider a combination of variables that would morph the wing outside of the aircraft's flight envelope, resulting in a nonclosure sizing case. Figure 2 shows the specific excess power of an aircraft as a function of velocity and aspect ratio for a given altitude. If the aircraft has positive $P_S$, it can maintain steady-level flight (SLF); in Fig. 2, not all values of AR can maintain SLF at this altitude.

For example, during the sizing process, the AR may have been nine at the end of the climb segment, and SLF is possible between about 650 and 810 ft/s. If the set of design variables then specified that AR = 5 for the subsequent cruise segment at the same altitude, SLF is not possible at any speed; this created the nonclosure cases. Realistically, the flight-control system and/or pilot would prevent operation at these conditions, but the sizing code and optimization problem formulation did not recognize this.

Introducing fictitious flight velocities indicative of best-available performance when the aircraft violated its flight envelope during analysis enabled continuous prediction of takeoff gross weight (the performance metric in this case) as a function of the design variables. Constraining specific excess power to be nonnegative during all mission legs ensured a feasible solution to the sizing problem.

Having a continuous design space enabled additional computational efficiency via a new problem formulation. Using a compatibility constraint in the optimization problem replaced the iteration for gross weight that typically occurs within the sizing code, and the initial guess for gross weight joined the design variable vector. Equations (6–12) demonstrate the refined problem statement.

Minimize:

$$f(\mathbf{x}) = W_0 \tag{6}$$

subject to

$$g_c(\mathbf{x}) = [W_0 - W_G(\mathbf{x})]^2 \leq \varepsilon \tag{7}$$

$$g_{j+i}(\mathbf{x}) = P_{S_i}(\mathbf{x}) \geq 0 \tag{8}$$

for $i = 1, m$

$$g_j(\mathbf{x}) = d_{\mathrm{TO}}(\mathbf{x}) \leq (d_{\mathrm{TO}})_{\mathrm{allow}} \tag{9}$$

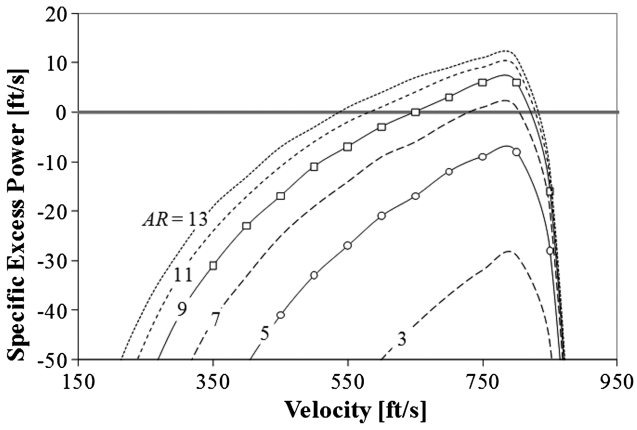


**Fig. 2 Specific excess power as a function of velocity for several different possible morphing-wing AR values.**

$$g_j(\mathbf{x}) = M_{\text{dash}}(\mathbf{x}) \geq (M_{\text{dash}})_{\min} \tag{10}$$

$$x_i^L \leq x_i \leq x_i^U \tag{11}$$

where

$$\mathbf{x} = \{ W_0 \;\; T_{\text{SL}}/W_0 \;\; S_1 \;\; S_2 \;\; \cdots \;\; S_m \;\; \text{AR}_1 \;\; \text{AR}_2 \;\; \cdots \;\; \text{AR}_m \;\; (t/c)_1 \;\; (t/c)_2 \;\; \cdots \;\; (t/c)_m \;\; \lambda_1 \;\; \lambda_2 \;\; \cdots \;\; \lambda_m \;\; \Lambda_1 \;\; \Lambda_2 \;\; \cdots \;\; \Lambda_m \} \tag{12}$$

The compatibility constraint [Eq. (7)] ensured that the gross weight design variable $W_0$ was nearly equal to the calculated gross weight $W_G$ at the solution; a small, positive $\varepsilon$ determines the tolerance between these two values. The problem now included $P_S \geq 0$ constraints for each mission leg along with any other performance constraints. For example, Eqs. (9) and (10) would constrain takeoff distance and dash Mach number. A gradient-based optimization algorithm, sequential quadratic programming (SQP) as available in MATLAB's fmincon, [30], replaced the GA and reduced the computational effort to a few hours on a PC. However, the approach restricted the wing shape to change only at the start of each mission leg to keep the number of design variables small.

### C. Morphing Aircraft Sizing via Multilevel Optimization

In addition to computational cost, the aforementioned efforts contained two features that limited their efficacy. First, describing the morphing-wing geometry with different independent variables for each mission leg resulted in a wing that changed shape without regard for a realizable morphing mechanism. Second, fixed-geometry wing weight predictors provided a basis for morphing-wing weight prediction in the previous work; additional empty weight based on the extent of wing shape change accounted for the underlying, yet undefined, morphing mechanism. This incremental morphing weight relied on a pound-per-square-foot heuristic for lack of a better model. To address these issues, Skillen and Crossley [31,32] developed a morphing-wing template strategy to model shape-change capabilities, which ultimately led to a multilevel optimization problem formulation for morphing aircraft sizing.

#### 1. Geometric Parameterization Approach to Define a Morphing Wing

The multilevel optimization problem formulation relies on the distinction of three major sets of variables to describe a morphing wing: 1) a set of variables, $\mathbf{X}^{\text{ref}}$, consisting of five of the basic six sizing variables, $S_{\text{ref}}$, $\text{AR}_{\text{ref}}$, $(t/c)_{\text{ref}}$, $\lambda_{\text{ref}}$, and $\Lambda_{\text{ref}}$, defining a reference wing geometry; 2) a set of variables $\boldsymbol{\xi}_k$ describing the amount of morphing from the reference wing geometry during design mission leg or segment $k$; and 3) a set of variables $\mathbf{X}^{\text{ub}}$ defining the maximum extent of morphing. The $\mathbf{X}^{\text{ref}}$ values are the minimum values that the morphing wing can attain during flight. The variables contained in $\boldsymbol{\xi}_k$ and $\mathbf{X}^{\text{ub}}$ depend upon the morphing strategy and are generally nondimensional, describing a maximum attainable percentage increase from the reference state. For example, $\boldsymbol{\xi}_k = \{\Delta\Lambda_k \Delta c_k \Delta b_k\}$ and $\mathbf{X}^{\text{ub}} = \{\Delta\Lambda_{\text{ub}} \Delta c_{\text{ub}} \Delta b_{\text{ub}}\}$ model a wing that could change sweep, chord, and span in some manner; if $\Delta c_{\text{ub}} = 0.2$, the morphing mechanism allows, at most, a 20% increase from chord length computed explicitly, or implicitly, from $\mathbf{X}^{\text{ref}}$, depending on the reference wing parameters contained in the set. In the aircraft sizing process, a top-level optimization problem uses $\mathbf{X}^{\text{ref}}$ and $\mathbf{X}^{\text{ub}}$ as part of its design variable vector, such that the top-level process controls the domain of achievable wing states. The sublevel problems then optimize a relevant metric for each mission leg (e.g., minimize fuel consumed in leg $k$) using that leg's $\boldsymbol{\xi}_k$ as the design variables.

#### 2. Morphing-Wing Template

The definitions of $\mathbf{X}^{\text{ref}}$ and $\mathbf{X}^{\text{ub}}$ 1) provide a lower bound to the morphing-wing shape based upon a reference geometry, 2) describe morphing variables that define geometric aspects of the wing controlled by the underlying actuation mechanism, and 3) define the maximum state these morphing variables can take. A full description of the morphing wing requires a means to determine intermediate states of the wing. This approach assumes that the actuation mechanism drives a smooth (or piecewise smooth) geometric transition of the wing. As such, intermediate states of the wing follow continuous or, at least, piecewise continuous functions of the morphing variables in $\boldsymbol{\xi}$. This continuity facilitates using a gradient-based optimization method for the multilevel search.

The morphing-wing template is a process that updates the wing-geometry parameters as a function of the current values in $\boldsymbol{\xi}_k$ (Fig. 3 depicts this process). The template uses the current values of values $\boldsymbol{\xi}_k$ with values of the reference wing-geometry variables $\mathbf{X}^{\text{ref}}$ to determine the wing geometry $\mathbf{Y}_k$ through a series of functions $\mathbf{F}()$ representing the effect of the morphing actuation scheme. This geometric description of the morphed wing $\mathbf{Y}_k$ includes all dimensions necessary to estimate lift and drag. Clearly, the functions $\mathbf{F}$ to compute $\mathbf{Y}_k$ are user developed and must match the morphing strategy under consideration. Reference [32] demonstrates formulation of several templates.

#### 3. Multilevel Optimization Architecture

The morphing aircraft sizing architecture has two levels: 1) a top-level problem that optimizes an aircraft-related objective and 2) a sizing routine consisting of several subproblems that optimize a performance objective for each mission leg. Equations (13–22) present the top-level optimization problem.

Minimize:

$$f(\mathbf{X}) = W_0 \tag{13}$$

subject to

$$g_c(\mathbf{X}) = W_G \leq W_0 \tag{14}$$

$$g_j(\mathbf{X}) = P_{S_k}(\mathbf{X}) \geq 0 \tag{15}$$

for $k = 1, m$

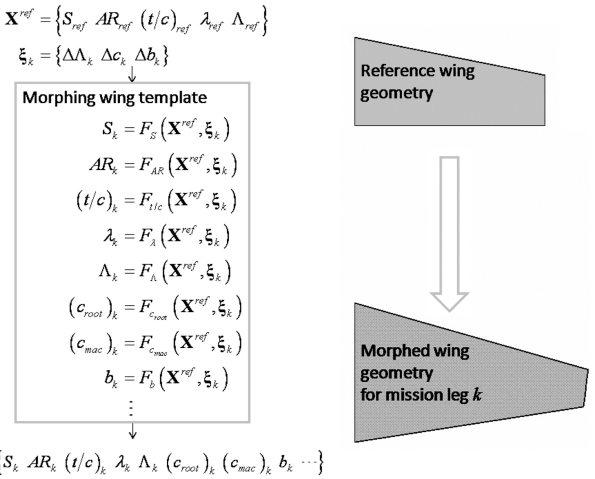


**Fig. 3 General definition of a morphing-wing template.**

$$g_j(\mathbf{X}) = C_{L_k}(\mathbf{X}) \leq (C_L)_{\max} \tag{16}$$

for $k = 1, m$

$$g_j(\mathbf{X}) = d_{\text{TO}}(\mathbf{X}) \leq (d_{\text{TO}})_{\text{allow}} \tag{17}$$

$$g_j(\mathbf{X}) = d_{\text{land}}(\mathbf{X}) \leq (d_{\text{land}})_{\text{allow}} \tag{18}$$

$$X_i^L \leq X_i \leq X_i^U \tag{19}$$

where

$$\mathbf{X} = \{ W_0 \quad T_{\text{SL}}/W_0 \quad \mathbf{X}^{\text{ref}} \quad \mathbf{X}^{\text{ub}} \} \tag{20}$$

where

$$\mathbf{X}^{\text{ref}} = \{ S_{\text{ref}} \quad \text{AR}_{\text{ref}} \quad (t/c)_{\text{ref}} \quad \lambda_{\text{ref}} \quad \Lambda_{\text{ref}} \} \tag{21}$$

and

$$\mathbf{X}^{\text{ub}} = \{ \Delta\Lambda_{\max} \quad \Delta c_{\max} \quad \Delta b_{\max} \} \tag{22}$$

The objective [Eq. (13)] is to minimize the takeoff gross weight of the aircraft $W_0$. The top-level problem includes flight envelope constraints (here, $P_S \geq 0$ and $C_L \leq (C_L)_{\max}$) and performance constraints such as maximum takeoff distance, maximum landing distance, etc., as presented by Eqs. (15–18). Flight envelope constraints exist for nearly all mission legs, so the number of these constraints will vary with the design mission being considered. The performance constraints will also vary in both number and type, depending upon the aircraft's mission requirements; hence, this general presentation of the problem does not have a numbering scheme for the index $j$, and the constraint set $\mathbf{g}_j$ is not exhaustive.

The top-level problem also uses a compatibility constraint [Eq. (14)] to ensure that the takeoff gross weight design variable value $W_0$ does not exceed the predicted takeoff gross weight $W_G$. Aircraft sizing requires an initial guess of takeoff gross weight to predict flight performance and fuel consumption; the variable $W_0$ provides this. If the initial guess weight of the aircraft exceeds the predicted takeoff gross weight, reducing $W_0$ will not adversely impact the other constraints. The compatibility constraint drives itself into the active set so that the difference between $W_0$ and $W_G$ is negligible for a feasible solution. This compatibility constraint replaces the weight iterations within a typical standalone aircraft sizing code.

The design variable vector $\mathbf{X}$ for this top-level problem contains thrust-to-weight ratio $T_{\text{SL}}/W_0$, the initial guess of takeoff gross weight $W_0$, the wing reference variables $\mathbf{X}^{\text{ref}}$, and the maximum wing shape-change values $\mathbf{X}^{\text{ub}}$. Equation (22) suggests a morphing wing

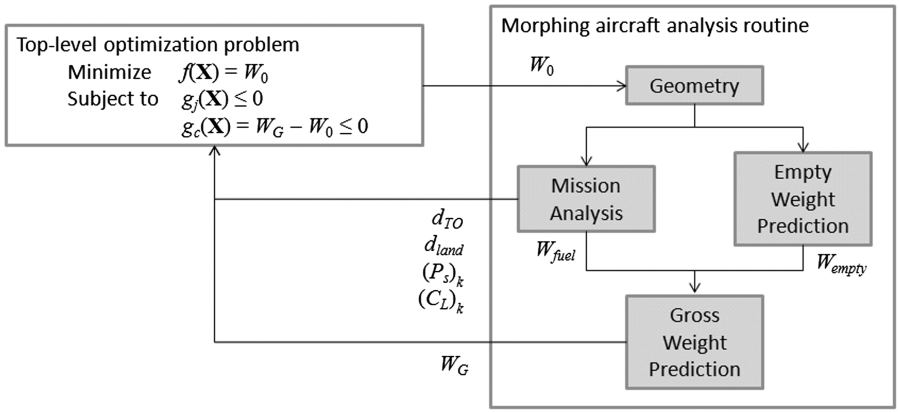


**Fig. 4 Top-level optimization problem interface with the morphing aircraft analysis routine.**

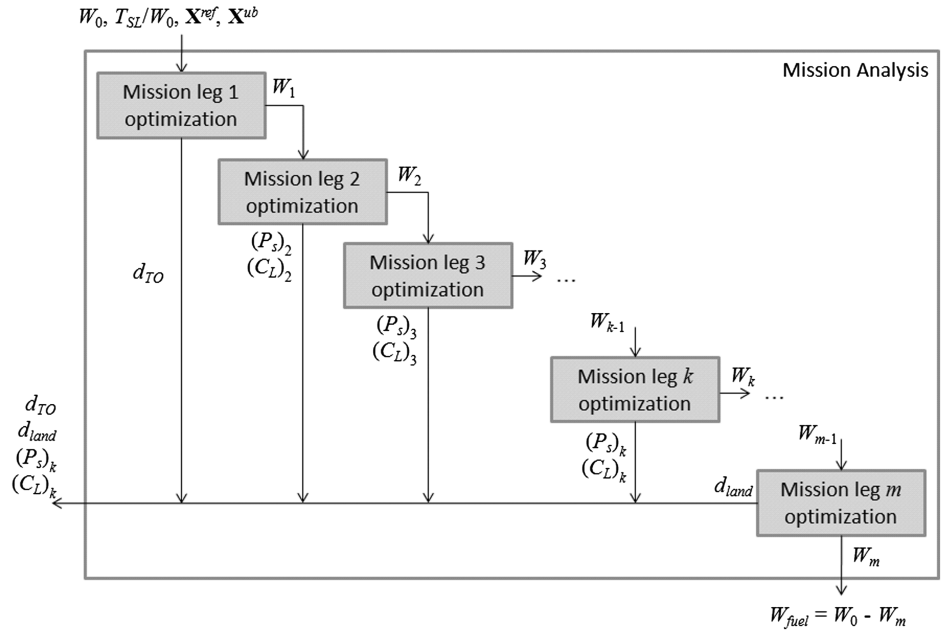


**Fig. 5 Information flow between the mission-leg optimization problems in the mission analysis portion of the morphing aircraft sizing routine.**

that could change sweep, chord, and span, but this set could change depending on the morphing strategy under consideration or on the parameterization of the morphed wing state.

For the implementations discussed in the following sections of this paper, the SQP algorithm in MATLAB's fmincon [30] solved the top-level problem.

The top-level objective and constraint function evaluations require values computed by the morphing aircraft sizing routine. To accomplish this, the sizing routine first uses the design variable values set by the top-level optimizer to establish the overall aircraft geometry. For this implementation, the length of the fuselage is a user-defined constant, and this establishes moment arm lengths from the wing to the horizontal and vertical tails; the aspect ratio, sweep, and thickness-to-chord ratio of the empennage are also user inputs and remain constant throughout the sizing routine. Using the volume coefficient method of [21], the horizontal and vertical tail areas are a function of the moment arm length, corresponding volume coefficient, and main wing geometry. Because a morphing aircraft's wing changes geometry during flight, the tail area calculations for the morphing aircraft use the wing state that maximizes the tail's size. For example, this approach calculates horizontal tail area using the maximum product of the main wing's mean aerodynamic chord and planform area. This may result in high stability margins during some flight legs but avoids unstable wing and tail area combinations, within the limits of the tail volume coefficient concept.

Using $W_0$ and the geometry of the aircraft, traditional component-weight predictors ([21], pp. 473–476) calculate the empty-weight contributions of all aircraft components, except the morphing wing. These equations generally rely upon a regression of historical aircraft data for their coefficients and exponents. There is no historical component data to establish a morphing-wing weight predictor (beyond variable sweep); however, strategies by Skillen and Crossley [33,34] and Skillen [35] provide predictors for morphing-wing weight as a function of the wing geometric parameters, extents of actuation, aircraft weight, and design load factors. Equation (23) is one type of morphing-wing weight predictor; this predicts the weight of a variable-root-chord/variable sweep morphing wing and presumes that the wing will encounter different, prescribed design load factors in different planform configurations. $\Delta\Lambda_{\text{ub}}$ and $\Delta c_{\text{root,ub}}$ are the maximum change in sweep angle and root chord length. This equation predicts that an increase in the actuation range of the wing increases the predicted wing weight. For example, a maximum sweep angle variation of 10° results in a wing weight about 1.05 times that of a nonvariable sweep wing; a $\Delta\Lambda_{\text{ub}}$ of 30° results in a multiplier of about 1.14.

$$W_{\text{wing}} = (0.0352W_G)\frac{S^{0.4516}(\text{AR})^{1.3520}(1+\lambda)^{0.7850}[1+(\Delta\Lambda_{\text{ub}}/90)]^{0.4524}[1+(\Delta c_{\text{root}})_{\text{ub}}]^{0.0252}}{(1+\cos\Lambda)^{4.8970}[100(t/c)]^{0.8870}[(W_0/S)/10]^{0.0045}} \tag{23}$$

With the vehicle geometry description, mission analysis models compute the aircraft's performance and fuel consumption during each leg; the aircraft's design fuel weight is the sum of fuel consumed in each leg. The calculated aircraft gross weight $W_G$ is the sum of the empty, fuel, and payload weights (assuming an unmanned aircraft, there is no crew weight). The $W_G$ value and performance constraint values from the individual mission-leg simulations return to the top-level optimization, which updates the top-level design variables based on finite-difference gradient information. This process iterates until the top-level optimization convergences. Figure 4 presents an overview of the top-level optimization problem and its interaction with the morphing aircraft analysis routine.

As presented in Fig. 4, the morphing aircraft sizing process has the same basic approach as a traditional sizing code for fixed-geometry aircraft. However, the mission analysis section predicts the total fuel consumed during the design mission in a manner deviating from the approach for fixed-geometry aircraft. Aircraft performance and fuel consumption assessment for each mission leg involves solving an independent optimization problem to determine a best-performance wing state; this feature results in the multilevel optimization approach. The information flow of the mission analysis appears in Fig. 5.

Each mission-leg optimization problem seeks a wing state $\boldsymbol{\xi}_k$ that optimizes some performance metric relevant to the leg; most commonly, this problem minimizes fuel consumed. The wing state $\boldsymbol{\xi}_k$ is restricted to bounds of zero and $\mathbf{X}^{\text{ub}}$, as prescribed by the top-level problem. The weight of the aircraft at the start of each mission leg is the weight computed at the end of the preceding leg. Each mission leg could incorporate a number of smaller segments when continuous (or piecewise continuous) morphing over some duration is thought to be beneficial. For instance, a constant-altitude constant-speed cruise might have several short-distance segments for more accurate computation of the fuel consumed using Breguet's range equation. In mission legs using this sort of discretization, each segment becomes an independent optimization problem that uses the preceding segment's wing state as the initial guess for the current segment. In this manner, the approach determines the optimal wing state over the mission leg, providing a time-history-like description of the morphing wing.

With the reference wing geometry and the morphing upper bounds set by the top-level optimization problem, the mission leg or segment sublevel optimization problems do not necessarily have a feasible domain when performance constraints are present. However, the mission analysis needs to report the best achievable performance for the entire design mission, even if a segment-level optimization problem does not find a feasible solution, because the top-level problem requires continuous functions to facilitate the design space search. This is similar to the need to handle nonclosure cases experienced in previous morphing aircraft sizing approaches [27,28]. To enable the return of best-available performance when a sublevel problem has no feasible solution, the mission-leg-level optimization problems use an objective function with a penalty approach similar to that of . This ensures that each mission-leg optimization finds a feasible solution, if one exists. If a feasible solution does not exist, the mission-leg-level problem still converges to the flight condition closest to the target requirements, and the violated performance constraint values return to the top-level optimization problem. Because the top-level problem enforces these performance constraints via inequality constraints, the top-level optimizer will determine a search direction that updates the reference geometry and/or upper-bound morphing limit values to approach a feasible solution, if one exists. The mission-leg optimization problems have the following form:

minimize

$$f_k(\boldsymbol{\xi}_k) = W_{\text{fuel}_k}(\boldsymbol{\xi}_k) + \sum_{j=1}^{n_{\text{con}}} \max\{0, [g_j(\boldsymbol{\xi}_k) + \varepsilon]\}^2 \tag{24}$$

subject to

$$0 \le (\xi_k)_i \le X_i^{\text{ub}} \tag{25}$$

where

$$\boldsymbol{\xi}_k = \{\, \Delta c_k \quad \Delta b_k \quad \Delta\Lambda_k \,\} \tag{26}$$

In this problem, the $g_j(\boldsymbol{\xi}_k)$ constraints addressed via the penalty function are the appropriate mission-leg-specific versions of

Eqs. (15–18). For instance, the takeoff leg problem would use the takeoff distance constraint, while a cruise segment would use the lift coefficient and specific excess power constraints. Because the objective function in Eq. (24) uses a quadratic exterior penalty form, the small positive-valued $\varepsilon$ provides a numerical cushion at the constraint boundaries to help ensure that the solution strictly satisfies the $g_j(\boldsymbol{\xi}_k)$ constraints. Equation (26) presumes a morphing wing that could change chord, span, and sweep [consistent with Eq. (22)] for the top-level problem. While the mission-leg problem does not have explicit inequality constraints, the bounds in the problem require a constrained optimization algorithm. As with the top-level problem, MATLAB's fmincon [30] solves each mission-leg optimization problem.

For mission legs defined as a series of subsegments, the constraint values returned to the top-level optimization do not necessarily need to include information from each subsegment; the routine chooses relevant information from this set. For example, a constant-altitude/constant-speed cruise only returns the $P_s$ value for the first subsegment of the leg, where meeting this constraint is most challenging.

## III. Application of Multilevel Optimization for Morphing Aircraft Sizing

The following studies demonstrate the preceding morphing aircraft sizing approach for a variable sweep/variable-root-chord morphing aircraft concept.

### A. Top-Level Morphing Aircraft Sizing Problem

The top-level optimization problem for this example follows Eqs. (13–22). To model the variable sweep/variable chord morphing wing similar to the realizable morphing changes presented in Fig. 1b), the top-level design variables are

$$\mathbf{X} = \{\, W_0 \quad T_{SL}/W_0 \quad S_{ref} \quad AR_{ref} \quad (t/c)_{ref} \quad (\Lambda_{LE})_{ref} \quad (\Delta\Lambda_{LE})_{ub} \quad (\Delta c_{root})_{ub} \,\} \tag{27}$$

This study assumes a transonic, unmanned aircraft with a roughly circular cross-section fuselage 60 ft in length and 5 ft in maximum diameter. The reference wing taper ratio is a constant value of 0.3, which is typical for transonic swept wings; the incorporated aerodynamic analyses used here do not have sufficient fidelity to address wing taper as a variable (e.g., these analyses do not compute spanwise lift distribution). The horizontal tail has a volume coefficient of 0.7, a leading-edge sweep of 35°, a taper ratio of 0.35, and an aspect ratio of 6. The vertical tail has a volume coefficient of 0.06, a leading-edge sweep of 35°, a taper ratio of 0.6, and an aspect ratio of 1.5. The aircraft incorporates two turbofan engines with a bypass ratio of five; an engine model provides values for thrust and fuel consumption as functions of Mach number, altitude, and throttle setting. This study does not address morphing of the inlets to improve engine performance.

Table 1 presents the upper and lower limits imposed upon the top-level design variables. The values here are the authors' attempt to bound a reasonable but not overly restrictive design space.

**Table 1 Top-level design variable bounds**

| Design variable | Bounds | |
|---|---|---|
| | Lower | Upper |
| $W_0$, lb | 20,000 | 40,000 |
| $T_{SL}/W_0$ | 0.3 | 0.8 |
| $S_{ref}$, ft$^2$ | 100 | 350 |
| $AR_{ref}$ | 5 | 12 |
| $(\Lambda_{LE})_{ref}$, ° | 5 | 30 |
| $(t/c)_{ref}$ | 0.06 | 0.18 |

### B. Sublevel (Mission Leg) Optimization Problems

For this study, each sublevel optimization problem seeks to minimize the fuel consumed during the mission leg and to meet appropriate performance and flight envelope constraints. Each sublevel optimization problem uses the two morphing design variables:

$$\boldsymbol{\xi} = \{\, \Delta\Lambda_{LE} \quad \Delta c_{root} \,\} \tag{28}$$

where $\Delta c_{root}$ is the percentage increase of the root chord length with respect to the reference configuration value (i.e., $\Delta c_{root} = 0.50$ indicates that the wing has increased its root chord length by 50% from the reference configuration root chord length). $\Delta\Lambda_{LE}$ is the leading-edge sweep angle increase with respect to the reference configuration value; $\Delta\Lambda_{LE}$ is normalized with respect to 90° to keep both sublevel variables on the same order of magnitude (i.e., $\Delta\Lambda_{LE} = 0.50$ indicates that the sweep has increased 45° from the reference sweep angle $\Lambda_{LE}$).

Table 2 summarizes the 10 design mission legs used for this variable sweep/variable-root-chord study. The altitudes and flight speeds are fixed parameters, and the optimization cannot change these values. All mission legs assume $(C_L)_{max} = 1.6$. For simplicity, the takeoff leg constraint uses a takeoff parameter (TOP) rather than distance:

$$\text{TOP} = \frac{W_0}{S} \Big/ \left[ \frac{(C_L)_{max}}{1.21} \frac{T_{SL}}{W_0} \right] \tag{29}$$

A TOP value of 155 corresponds to a balanced field length approximately 5500 ft for a twin-engine aircraft [21]. Also, for simplicity, the descent legs are no range credit. The multilevel optimization approach could handle other types of mission legs (e.g., payload drop, best-range cruise, etc.), other constraints, and other methods to compute field lengths without change to the basic algorithm construct.

**Table 2 Morphing aircraft design mission used to demonstrate the multilevel sizing approach**

| Leg | Type | Altitude, ft | Description | Constraints |
|---|---|---|---|---|
| 1 | Taxi, takeoff | 0 | | TOP $\leq$ 155 |
| 2 | Climb | 0 to 30,000 | Best rate of climb | $P_s \geq 0$, $C_L \leq (C_L)_{max}$ |
| 3 | Cruise | 30,000 | $M = 0.7$, range = 1500 n mile | $P_s \geq 0$, $C_L \leq (C_L)_{max}$ |
| 4 | Loiter | 30,000 | Endurance = 4 h | $P_s \geq 0$, $C_L \leq (C_L)_{max}$ |
| 5 | Descend | 30,000 to 5000 | No range credit | |
| 6 | Dash | 5,000. | $M = 0.8$, distance = 250 n mile | $P_s \geq 0$, $C_L \leq (C_L)_{max}$ |
| 7 | Climb | 5000 to 20,000 | Best rate of climb | $P_s \geq 0$, $C_L \leq (C_L)_{max}$ |
| 8 | Cruise | 20,000 | $M = 0.7$, range = 1500 n mile | $P_s \geq 0$, $C_L \leq (C_L)_{max}$ |
| 9 | Descend | 20,000 to 0 | No range credit | |
| 10 | Land, taxi | 0 | $V_{approach} = 1.2V_{stall}$ | Landing distance $\leq$ 5500 ft |

**Table 3 Initial and optimal design variable values with $\mathbf{X}^{ub}$ constant, $\{(\Delta c_{root})_{ub} = 0.95, (\Delta \Lambda_{LE})_{ub} = \frac{1}{3}\}$**

| Design variable | $\mathbf{X}^0$ | $\mathbf{X}^*$ |
|---|---|---|
| $W_0$, lb | 30,000 | 28,152 |
| $T_{SL}/W_0$ | 0.55 | 0.51 |
| $S_{ref}$, ft$^2$ | 325.00 | 155.74 |
| $AR_{ref}$ | 7.00 | 12.00 |
| $(t/c)_{ref}$ | 0.12 | 0.15 |
| $(\Lambda_{LE})_{ref}$, ° | 18.5 | 10.3 |

### C. Sizing Results Using Constant Upper Bounds on Morphing Variables

This first study demonstrates a simplified morphing aircraft sizing run. Here, the values of the morphing upper bounds $\mathbf{X}^{ub}$ are constant, so the top-level design variables include $W_0$, $T_{SL}/W_0$, and the reference wing-geometry variables $S_{ref}$, $AR_{ref}$, $(\Lambda_{LE})_{ref}$, and $(t/c)_{ref}$. With $\mathbf{X}^{ub}$ constant, the morphing-wing weight predictor prescribes a constant-percentage weight increment due to the morphing range of motion. This is important, because the added mechanism weight required to enable actuation to the $\mathbf{X}^{ub}$ values might result in extra empty weight if the wing never operates at these upper-bound wing states. The final study appearing later in this paper added $\mathbf{X}^{ub}$ as top-level design variables to size the aircraft with optimal morphing capabilities.

In this initial study, the morphing wing can increase its sweep aft by 30° from the reference sweep angle, $(\Delta\Lambda_{LE})_{ub} = 0.3333$, and can produce a 95% increase in root chord length, $(\Delta c_{root})_{ub} = 0.95$. Table 3 shows the initial and the computed optimal design variable values.

Figure 6 provides simple planform views of the aircraft at the beginning of each design mission leg. In this figure, the values of $\boldsymbol{\xi}_k^*$ from the mission-leg optimization problem follow each leg title. For example, during the leg 3 cruise, wing sweep changes $(\Delta\Lambda_{LE})_3 = 0$, and the root chord changes $(\Delta c_{root})_3 = 0.619$. The takeoff and landing configurations morph the wing to a large planform area, and the wing has a large sweep angle during the dash leg; these follow expected trends. With no range credit descents, there is no fuel weight to minimize, so the figure omits legs 5 and 9.

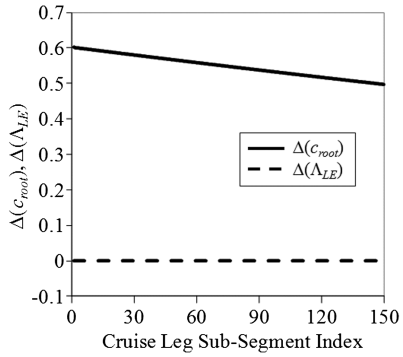


**Fig. 7 Wing-shape history during the first cruise leg.**

For this study, the cruise legs used 150 subsegments, each 100 n mile long. Figure 7 illustrates an example of the wing-shape history during the first cruise leg of the design mission by presenting the optimal morphing design variable values for each cruise subsegment; for these subproblems, the objective function convergence tolerance was $1 \times 10^{-4}$. During the first cruise leg, the wing sweep morphing variable is zero for all subsegments, so the sweep remains at the reference value (i.e., $\Lambda_{LE} = 10.3°$). The root chord morphing variable begins the mission leg at ~60% but reduces almost linearly to a value of ~50%. As the aircraft burns fuel, the wing root chord decreases. This decreases wing area and increases aspect ratio, because the wingspan does not change. This changing combination of wing loading and aspect ratio matches the specified cruise speed ($M = 0.7$) to the aircraft's best-range cruise speed. This is analogous to a cruise-climb; here, at a fixed altitude and cruise speed, the morphing aircraft performs a cruise shrink.

### D. Parametric Study of Morphing Upper Bounds on Aircraft Weight and Installed Thrust

This second study is similar to the previous one, in that $\mathbf{X}^{ub}$ remain constant during the process. Here, the approach sizes the morphing aircraft for different combinations of the prescribed $\mathbf{X}^{ub}$ values. This enables some visualization of the design space, showing the effect of

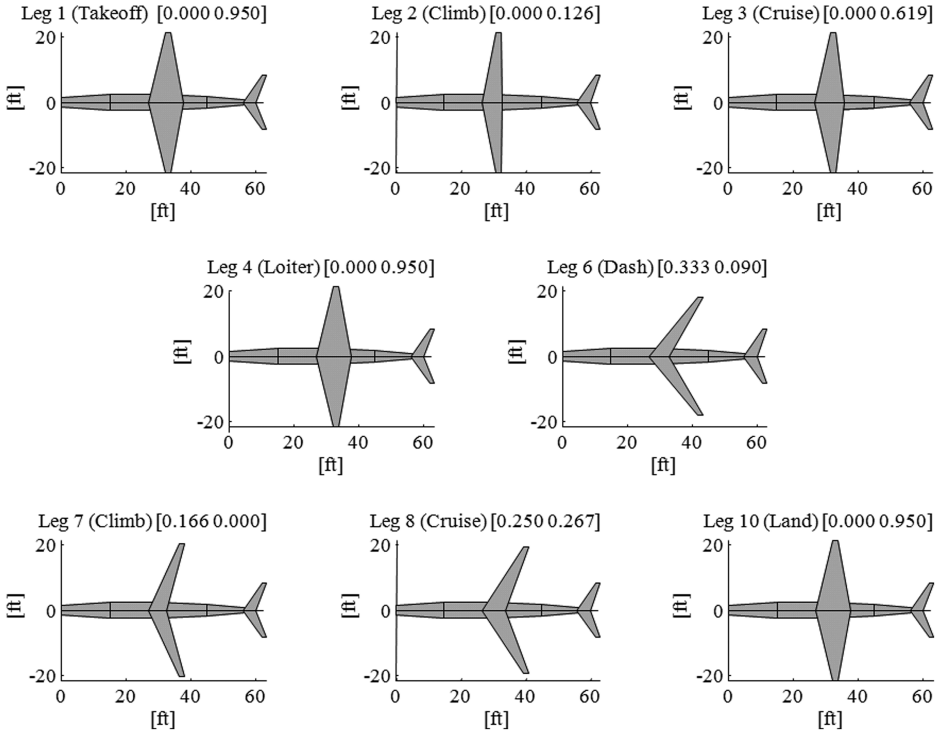


**Fig. 6 Planform views of the wing at the beginning of each design mission leg.**

**Table 4 Predicted $W_G$ for combinations of $(\Delta\Lambda_{LE})_{ub}$ and $(\Delta c_{root})_{ub}$**

| | $(\Delta\Lambda_{LE})_{ub}$ | | |
|---|---|---|---|
| $(\Delta c_{root})_{ub}$ | 1°, lb | 15°, lb | 30°, lb |
| 0.05 | 26,600 | 25,877 | 25,672 |
| 0.35 | 26,744 | 26,455 | 26,331 |
| 0.65 | 27,572 | 27,307 | 27,199 |
| 0.95 | 28,561 | 28,307 | 28,152 |

**Table 5 Installed thrust for combinations of $(\Delta\Lambda_{LE})_{ub}$ and $(\Delta c_{root})_{ub}$**

| | $(\Delta\Lambda_{LE})_{ub}$ | | |
|---|---|---|---|
| $(\Delta c_{root})_{ub}$ | 1°, lb | 15°, lb | 30°, lb |
| 0.05 | 12,559 | 12,223 | 12,125 |
| 0.35 | 12,864 | 12,893 | 12,702 |
| 0.65 | 13,548 | 13,597 | 13,739 |
| 0.95 | 14,394 | 14,303 | 14,264 |

$\mathbf{X}^{ub}$ on the reported optimal $W_G$ and maximum installed thrust values.

Tables 4 and 5 present the takeoff gross weight and maximum installed thrust values for various combinations of the morphing threshold values, and Figs. 8 and 9 provide graphical visualizations of the same data. $(\Delta\Lambda_{LE})_{ub}$ has three discrete values (1, 15, and 30° of sweep variation), while the $(\Delta c_{root})_{ub}$ parameter has four discrete values (0.05, 0.35, 0.65, and 0.95). For the 12 $\mathbf{X}^{ub}$ combinations, the morphing aircraft sizing process generated an aircraft description, each of which was a feasible design. A typical run required ~2 h to complete, using MATLAB on a dedicated PC with a 2.8 GHz Pentium IV processor.

The lowest $W_G$ and installed thrust occurred with $(\Delta\Lambda_{LE})_{ub} = 30°$ and $(\Delta c_{root})_{ub} = 0.05$. For this design mission (Table 2) and corresponding morphing-wing weight predictor [Eq. (23)], these results suggest that any aerodynamic performance improvements enabled by root chord variation to reduce fuel weight degrade the system-level metrics because of increasing empty weight (here, $W_G$ and installed thrust both increase). However, sweep variation improves the system-level metrics. This does not suggest that root chord variation is generally a poor morphing-wing design characteristic, but for the design mission and wing weight predictor used here, the variable root chord does not provide system-level benefits.

### E. Sizing Results with Morphing Parameters in Top-Level Design Variables

For this last study, the top-level design variables include $\mathbf{X}^{ub}$. These morphing variable upper bounds are free to span the values of

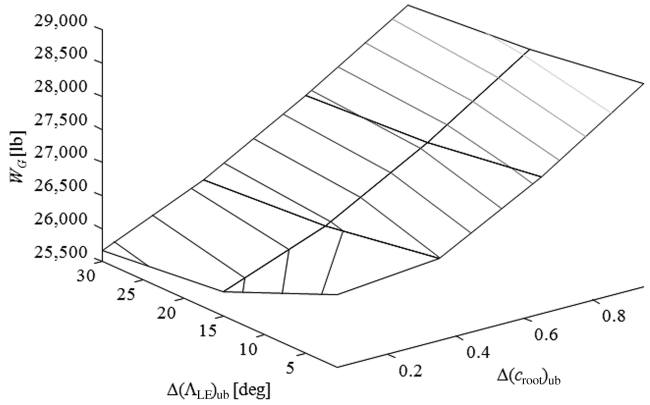


**Fig. 8 Predicted minimum takeoff gross weight for combinations of $(\Delta\Lambda_{LE})_{ub}$ and $(\Delta c_{root})_{ub}$.**

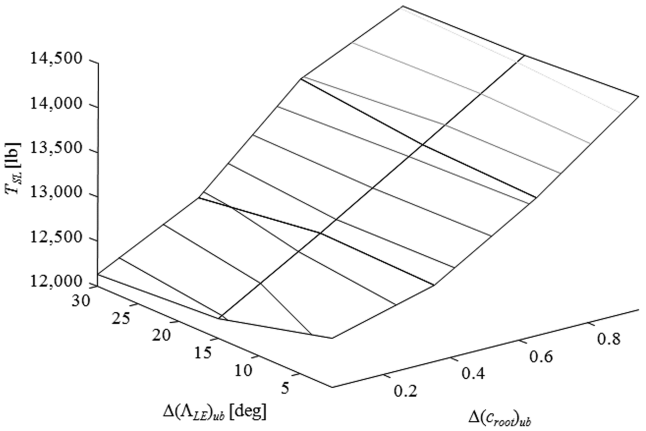


**Fig. 9 Installed thrust for combinations of $(\Delta\Lambda_{LE})_{ub}$ and $(\Delta c_{root})_{ub}$.**

the previous case study; $\Delta\Lambda_{LE,ub}$ is between a 1 and 30° increase, and $\Delta c_{root,ub}$ is between 0.05 and 0.95. The study used three different sets of initial design variable values to help verify a near-global optimum result. Table 6 shows the optimal design variable values obtained from each set of initial conditions; for the three runs, the initial values of $\mathbf{X}^{ub}$ are different. There are slight differences in the reference values of $S$, AR, and $\Lambda_{LE}$, but the gross weight of all the results are nearly the same. The runtimes for each of these sizing studies required about 2 h each, which is nearly consistent with the previous sizing studies that excluded the morphing upper bounds design variables.

Figure 10 revisits the plot from Fig. 8 and illustrates three initial morphing-parameter threshold values (shown as circles) and the optimal values (shown as an $X$) determined by the aircraft sizing routine. The solution has converged to the values enabling the lowest predicted $W_G$. This is encouraging, because it suggests the design space is smooth and the problem is well conditioned.

## IV. Limitations and Opportunities for Future Work

This paper presented several approaches for morphing aircraft sizing, and the studies with the multilevel optimization approach show that this appears to be the best approach for sizing a morphing aircraft. However, some aspects of the method presented here were restricted for demonstration of the approach and provide opportunities for future work.

Improvements to the representation of the morphing aircraft could better refine the results. As presented in this paper, the morphing only changes the wing planform. Strategies and mechanisms to change the wing airfoil shape (e.g., camber) and twist are viable options not investigated here; these changes could improve the aerodynamic performance of the aircraft throughout a design mission. To address these changes, the wing weight prediction scheme would require an update or, possibly, a completely new prediction scheme. The stability and control of the aircraft is also a concern, especially as changing wing planform will likely move the aircraft's center of lift; some consideration beyond the tail volume coefficient would improve this aspect of the resulting designs. The design mission used in the illustrative studies combined efficient cruise legs with a reasonably long-endurance loiter and a reasonably high-speed dash, making the use of a morphing wing beneficial. The previously presented studies used a set of tabular engine data in a rubber engine approach (i.e., sea-level static thrust scaling); however, these engine data reflect a presumed inlet and nozzle and a somewhat limited envelope of operating altitudes and Mach numbers. For missions combining vastly dissimilar performance requirements in different mission legs (e.g., a high-altitude long-endurance loiter and a low-altitude supersonic dash), an engine model that covers a wider range of flight conditions becomes necessary. Similarly, morphing of the inlet and or nozzle may also facilitate the wider range of flight conditions.

**Table 6 Optimal design variable values for various initial conditions**

| | Trial 1 | | Trial 2 | | Trial 3 | |
|---|---|---|---|---|---|---|
| Design variable | $\mathbf{X}^0$ | $\mathbf{X}^*$ | $\mathbf{X}^0$ | $\mathbf{X}^*$ | $\mathbf{X}^0$ | $\mathbf{X}^*$ |
| $W_0$, lb | 30,000.00 | 25,691.51 | 30,000.00 | 25,691.84 | 30,000.00 | 25,659.09 |
| $T_{SL}/W_0$ | 0.55 | 0.47 | 0.55 | 0.47 | 0.55 | 0.47 |
| $S_{ref}$, ft$^2$ | 225.00 | 197.86 | 225.00 | 203.92 | 225.00 | 195.96 |
| $AR_{ref}$ | 8.50 | 11.91 | 8.50 | 11.99 | 8.50 | 12.00 |
| $(\Lambda_{LE})_{ref}$, ° | 17.50 | 10.3 | 17.50 | 13.2 | 17.50 | 12.0 |
| $(t/c)_{ref}$ | 0.12 | 0.14 | 0.12 | 0.14 | 0.12 | 0.15 |
| $(\Delta\Lambda_{LE})_{ub}$, ° | 1.00 | 30.00 | 1.00 | 30.00 | 15.00 | 29.93 |
| $(\Delta c_{root})_{ub}$ | 0.05 | 0.0536 | 0.95 | 0.0510 | 0.50 | 0.0500 |

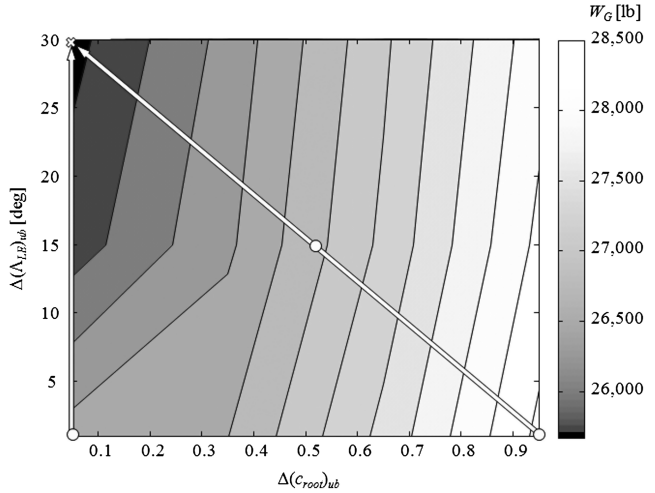


**Fig. 10 Initial and final values of $(\Delta\Lambda_{LE})_{ub}$ and $(\Delta c_{root})_{ub}$ superposed on TOGW contours.**

Different design missions and performance constraints will likely result in different morphing strategies. Here, the result that substantially changing the root chord of the wing is not beneficial may change if the design mission included requirements for extremely short takeoff or landing, or for high-$g$ maneuver capabilities. Also, the fidelity used in the analysis is reasonable but somewhat simplistic. For instance, the current studies do not address the aerodynamic effect of changing taper ratio; as $c_{root}$ changed, $S$, $c_{mac}$, and $\lambda$ changed. However, the aerodynamic analyses only accounted for changes in $S$ and $c_{mac}$.

## V. Conclusions

This paper presented a sequence of approaches to size morphing aircraft. The early efforts established the notion that the wing planform description in each mission leg should be design variables and identified the need to enforce flight envelope constraints [i.e., $P_s \geq 0$ and $C_L \leq (C_L)_{max}$], but these early efforts did not provide the necessary efficiency for morphing aircraft sizing studies. The development of these approaches culminated in an approach that has the necessary features for sizing morphing aircraft.

The key aspect of this approach is the multilevel optimization formulation. A top-level problem controls variables that describe a reference wing geometry and variables that describe the upper bounds on the geometric change available from a morphing strategy [e.g., $(\Delta\Lambda_{LE})_{ub}$ and $(\Delta c_{root})_{ub}$ for the previously presented studies]. The prediction of aircraft empty weight is a function of the upper bounds on the planform change. To predict the fuel consumed over the design mission, the morphing aircraft sizing approach addresses each leg of the mission via one (or more) constrained optimization subproblem(s). Each of these subproblems minimizes the fuel consumed during the mission leg by varying the wing geometry within the bounds set by the limits on the morphing variable values from the top-level problem. Constraints imposed on each mission-leg subproblem ensure that the aircraft remains within its flight envelope and does not require a lift coefficient that exceeds $(C_L)_{max}$. A penalty formulation for the subproblems' objective functions allows the top-level optimization to proceed when there are no feasible solutions to a mission-leg subproblem. By increasing the number of subsegments in each mission leg, this approach represents continuous morphing during the mission leg, as demonstrated by the cruise-shrink behavior of the wing. Previous morphing aircraft sizing approaches did not incorporate this major feature.

The multilevel optimization approach enables rapid conceptual studies of morphing aircraft concepts. Based on the case studies, the problem formulation appears well conditioned. A complete design run requires on the order of 2 h; these runs used a dedicated computer with a Pentium IV processor (2.8 GHz), running Windows XP and MATLAB 7.1 (R14).

## Acknowledgments

The work presented here combined portions of several different efforts; these include grants NAG-1-01115 and NNL06AA04G, from NASA Langley Research Center, and contract F33615-00-C3051, from the U.S. Air Force Research Laboratory Air Vehicles Directorate. A NASA Graduate Student Researcher Program award provided support for the second author.

## References

[1] DeCamp, R. W., and Hardy, R., "Mission Adaptive Wing Advanced Research Concepts," AIAA Paper 1984-2008, Aug. 1984.

[2] Pitt, D. M., Dunne, J. P., and White, E. V., "SAMPSON Smart Inlet Design Overview and Wind Tunnel Test Part I: Design Overview," *Proceedings of the SPIE: Smart Structures and Materials 2002, Industrial and Commercial Applications of Smart Structures Technologies*, edited by A.-M. R. McGowan, Vol. 4698, SPIE, Bellingham, WA, 2002, pp. 13–23.

[3] Wlezien, R. W., Horner, G. C., McGowan, A. R., Padula, S. L., Scott, M. A., Silcox, R. J., and Simpson, J. O., "The Aircraft Morphing Program," AIAA Paper 1998-1927, Apr. 1998.

[4] McGowan, A. R., Washburn, A. E., Horta, L. G., Bryant, R. G., Cox, D. E., Siochi, E. J., Padula, S. L., and Holloway, N. M., "Recent Results from NASA's Morphing Project," SPIE Paper 4698-11, Bellingham, WA, Mar. 2002.

[5] Kudva, J., "Overview of the DARPA Smart Wing Project," *Journal of Intelligent Material Systems and Structures*, Vol. 15, No. 4, Apr. 2004, pp. 261–267. doi:10.1177/1045389X04042796

[6] Wall, R., "DARPA Eyes Materials for 'Morphing' Aircraft," *Aviation Week and Space Technology*, Vol. 156, No. 15, April 2002, p. 36.

[7] Hetrick, J. A., Osborn, R. F., Kota, S., Flick, P. M., and Paul, D. B., "Flight Testing of Mission Adaptive Compliant Wing," AIAA Paper 2007-1709, April 2007.

[8] Love, M. H., Zink, P. S., Stroud, R. L., Bye, D. R., and Chase, C., "Impact of Actuation Concepts on Morphing Aircraft Structures," AIAA Paper 2004-1724, Apr. 2004.

[9] Ivanco, T. G., Scott, R. C., Love, M. H., Zink, S., and Weisshaar, T. A., "Validation of the Lockheed Martin Morphing Concept with Wind Tunnel Testing," AIAA Paper 2007-2235, April 2007.

[10] Bowman, J., Sanders, B., Cannon, B., Kudva, J., Joshi, S., and Weisshaar, T., "Development of Next Generation Morphing Aircraft Structures," AIAA Paper 2007-1730, April 2007.

[11] Warwick, G., "NextGen's Shape-Changing UAV Morphs in Flight," *Flightglobal* [online journal], Oct. 2007, http://www.flightglobal.com/articles/2007/10/19/218799/nextgens-shape-changing-uav-morphs-in-flight.html [retrieved 20 April 2010].

[12] Lu, K.-J., and Kota, S., "Design of Compliant Mechanisms for Morphing Structural Shapes," *Journal of Intelligent Material Systems and Structures*, Vol. 14, No. 6, 2003, pp. 379–391. doi:10.1177/1045389X03035563

[13] Saggere, L., and Kota, S., "Static Shape Control of Smart Structures Using Compliant Mechanisms," *AIAA Journal*, Vol. 37, No. 5, 1999, pp. 572–578. doi:10.2514/2.775

[14] Vos, R., DeBreuker, R., Barrett, R., and Tiso, P., "Morphing Wing Flight Control via Postbuckled Precompressed Piezoelectric Actuators," *Journal of Aircraft*, Vol. 44, No. 4, 2007, pp. 1060–1068. doi:10.2514/1.21292

[15] Blondeau-Samuel, J., and Pines, D., "Design and Testing of a Pneumatic Telescopic Wing for Unmanned Aerial Vehicles," *Journal of Aircraft*, Vol. 44, No. 4, 2007, pp. 1088–1099. doi:10.2514/1.22205

[16] Sofla, A. Y. N., Meguid, S. A., Tan, K. T., and Yeo, W. K., "Shape Morphing of Aircraft Wing: Status and Challenges," *Materials and Design*, Vol. 31, No. 3, 2010, pp. 1284–1292. doi:10.1016/j.matdes.2009.09.011

[17] Bowman, J., Sanders, B., and Weisshaar, T., "Evaluating the Impact of Morphing Technologies on Aircraft Performance," AIAA Paper 2002-1631, April 2002.

[18] Bye, D. R., and McClure, P. D., "Design of a Morphing Vehicle," AIAA Paper 2007-1728, April 2007.

[19] Joshi, S. P., Tidwell, Z., Crossley, W. A., and Ramakrishnan, S., "Comparison of Morphing Wing Strategies Based upon Aircraft Performance Impacts," AIAA Paper 2004-1722, April 2004.

[20] Raymer, D., "Vehicle Scaling Laws for Multidisciplinary Optimization," AIAA Paper 2001-0532, Jan. 2001.

[21] Raymer, D., *Aircraft Design: A Conceptual Approach*, 3rd ed., AIAA Education Series, AIAA, Reston VA, 1999.

[22] Sobieski, I., and Kroo, I., "Aircraft Design using Collaborative Optimization," *34th Aerospace Sciences Meeting and Exhibit*, Reno, NV, AIAA Paper 1996-715, Jan. 1996.

[23] Kroo, I., Altus, S., Braun, R., Gage, P., and Sobieski, I., "Multidisciplinary Optimization Methods for Aircraft Preliminary Design," AIAA Paper 1994-4325, Sept. 1994.

[24] Sobieszczanski-Sobieski, J., Agte, J. S., and Sandusky, R. R., "Bilevel Integrated System Synthesis," *AIAA Journal*, Vol. 38, No. 1, 2000, pp. 164–172. doi:10.2514/2.937

[25] Gallman, J., Kaul, R., Chandrasekharan, R., and Hinson, M., "Optimization of an Advanced Business Jet," *Journal of Aircraft*, Vol. 34, No. 3, May–June 1997, pp. 288–295. doi:10.2514/2.2197

[26] Roth, B., Peters, C., and Crossley, W., "Aircraft Sizing with Morphing as an Independent Variable: Motivation, Strategies, and Investigations," AIAA Paper 2002-5840, Oct. 2002.

[27] Roth, B., and Crossley, W., "Application of Optimization Techniques in the Conceptual Design of Morphing Aircraft," AIAA Paper 2003-6733, Nov. 2003.

[28] Frommer, J., and Crossley, W., "Enabling Continuous Optimization for Sizing Morphing Aircraft Concepts," AIAA Paper 2005-0816, Jan. 2005.

[29] Skillen, M. D., and Crossley, W. A., "Conceptual Morphing Aircraft Sizing Using a Multi-Level Optimization Strategy," AIAA Paper 2008-0166, Jan. 2008.

[30] MATLAB, Software Package, Ver. 7.1.0.246, Release 14, The MathWorks, Inc., Natick, MA, 2005.

[31] Skillen, M. D., and Crossley, W. A., "Modeling and Optimization for Morphing Wing Concept Generation," NASA CR 2007-214860, 2007.

[32] Skillen, M. D., and Crossley, W. A., "Modeling and Optimization for Morphing Wing Concept Generation II, Part I: Morphing Wing Modeling and Structural Sizing Techniques," NASA CR 2008-214902, Feb. 2008.

[33] Skillen, M., and Crossley, W., "Developing Response Surface Based Wing Weight Equations for Conceptual Morphing Aircraft Sizing," AIAA Paper 2005-1960, April 2005.

[34] Skillen, M., and Crossley, W., "Developing Morphing Wing Weight Predictors with Emphasis on the Actuating Mechanism," AIAA Paper 2006-2042, May 2006.

[35] Skillen, M., "Developing Response Surface Based Wing Weight Equations for Conceptual Morphing Aircraft Sizing," M.S. Thesis, School of Aeronautics and Astronautics, Purdue Univ., West Lafayette, IN, Dec. 2005.

[36] deMiguel, A.-V., and Murray, W., "Two Decomposition Algorithms for Nonconvex Optimization Problems with Global Variables," Stanford University, Department of Management Science and Engineering, TR SOL 01-1, Stanford, CA, 2001.

[37] Toensmeier, P. A., "Radical Departure: Morphing Structures Could Bring Multi-Role Capabilities to Next-Generation Aircraft," *Aviation Week and Space Technology*, Vol. 162, No. 21, May 2005, pp. 72–73.

[38] Wall, R., "Taking Shape: DARPA Sees Progress in Shape-Changing Unmanned Aircraft and Missiles," *Aviation Week and Space Technology*, Vol. 160, No. 1, Jan. 2004, pp. 54–56.